DØ - note 5047-Conf

Measurement of $m_{\rm top}$ in Dilepton Events with Neutrino Weighting in Run II at DØ

The DØ Collaboration
URL http://www-d0.fnal.gov
(Dated: March 10, 2006)

We present a measurement of the mass of the top quark, $m_{\rm top}$, in dilepton final states from top pair production. We utilize expected neutrino rapidity distributions to solve the otherwise underconstrained kinematic fit. A data sample of approximately 370 pb^{-1} of DØ Run II data in the $e\mu$, ee, and $\mu\mu$ channels is used for this analysis. The top quark mass extracted from 21 dilepton candidate events is measured to be:

$$m_{top}^{\ell\ell} = 175.6 \pm 10.7(\text{stat.}) \pm 6.0(\text{syst.}) \text{ GeV}.$$

Preliminary Results for Winter 2006 Conferences

Contents

I. INTRODUCTION

In the standard model, mass is generated from the spontaneous breaking of electroweak symmetry via the Higgs mechanism. A precision measurement of the mass of the top quark provides information about the Higgs boson mass via corrections to the W boson mass. In this analysis, the top quark mass is measured in dilepton decays of $t\bar{t}$ events; that is, events in which each top quark decays to a b quark and a W boson, and in which each W boson in turn decays leptonically.

The top quark mass is measured for events collected at DØ between April 2002 and August 2004 of Run II at the Tevatron, comprising approximately 360 pb^{-1} of data. The DØ detector is described in detail in [1]. The mass is measured from candidate events in the dielectron (ee), electron+muon ($e\mu$), and dimuon ($\mu\mu$) channels.

II. METHOD

In dilepton decays, the final state consists of six particles: two leptons, two jets from b quarks, and two neutrinos. The mass of each final particle is known *a priori*, so this results in 18 independent kinematic quantities in the final state. Fourteen of these parameters – the momenta of the leptons and jets and the transverse energy components of the neutrino pair – are measured directly in the detector. Three additional constraints are added by requiring that the invariant mass of each lepton and neutrino pair equal the W mass and that the mass of the top and anti-top quarks be equal. This leads to a total of seventeen constraints, which is one constraint short of allowing a solution for the system.

A solution is found by ignoring the observed missing transverse energy ($\not\!\!E_T$) from the neutrinos and instead assuming a top quark mass and a pseudorapidity [2] for each neutrino. From this information, the four-momentum of each neutrino may be determined. The measured missing energy is then used to assign a weight to the solution, based on the agreement of the calculated transverse momentum of the neutrinos with the observed missing transverse energy ($\not\!\!E_T$):

$$\omega = \frac{1}{N_{iter}} \sum_{i=1}^{N_{iter}} \exp\left(\frac{-(\not\!\!E_{x,i}^{calc} - \not\!\!E_x^{obs})^2}{2\sigma_{E_x}^2}\right) \exp\left(\frac{-(\not\!\!E_{y,i}^{calc} - \not\!\!E_y^{obs})^2}{2\sigma_{E_y}^2}\right) \tag{1}$$

.

This procedure is repeated for 10 pseudorapidity choices of each neutrino at the assumed top quark mass, and a weight is formed by summing over the weights for each neutrino choice. At each mass, the jets and lepton momenta are smeared 150 times within detector resolutions, and the solution algorithm is repeated for each smearing. The weights for all smearings are summed together to form a total event weight at the assumed top quark mass. Weights are generated in 2 GeV increments for top quark masses between 80 and 330 GeV. When these weights are summed over a large number of Monte Carlo events, they produce a peak near the input top quark mass, as shown in Figure 1.

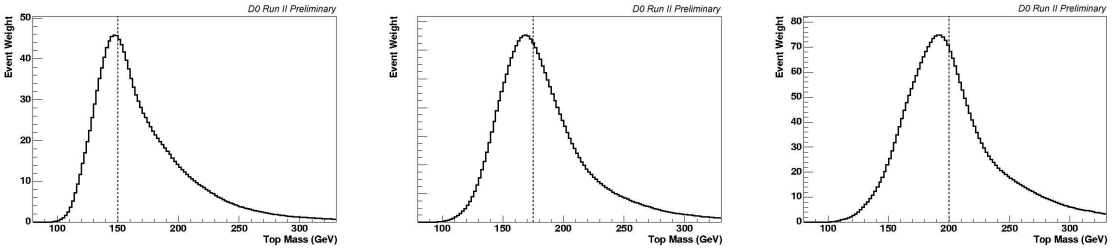

(a) (b) (c)

FIG. 1: Sum of event weights for a few thousand $t\bar{t}$ Monte Carlo events with top quark mass of (a) 150, (b) 175, and (c) 200 GeV. The dashed vertical lines indicate the mass of the Monte Carlo top quarks.

III. EVENT SELECTION

Dilepton events from the 360 pb^{-1} data set are sorted according to the type of leptons found in the event ($e\mu$, ee, or $\mu\mu$) Events are required to pass a Level 1 dilepton trigger as well as a Level 2 ($\mu\mu$) or Level 3 (ee, $e\mu$) trigger. All events are required to

pass the selection criteria of the dilepton cross section analyses described in [3]. These analyses require two oppositely-charged leptons with $p_T > 15$ GeV and two jets with $p_T > 20$ GeV, as well as significant total energy from the jets and leading lepton (H_T^ℓ) in the event. Channel-dependent cuts are applied to reduce physics and instrumental backgrounds.

The selection for the *ee* and $\mu\mu$ channels is identical to the cross-section analysis selection for those channels. The dominant background in both channels comes from $Z->\ell\ell$ decays in which extra jets are present and in which there is significant "fake" missing transverse energy ($\not\!\!E_T$) from instrumental sources. These backgrounds are reduced by applying cuts to the dilepton mass ($M_{\ell\ell}$) in each channel. In the *ee* channel, events must also have a sphericity greater than 0.15, where sphericity is defined as in [4]. This serves to reduce backgrounds due to gluon radiation. In the $\mu\mu$ channel, events in which the muon p_T is severely mismeasured are removed by applying a contour cut on $\not\!\!E_T$. This cut eliminates events in which the azimuthal angle between the leading muon and $\not\!\!E_T$ is greater than 175°. The remaining events must have $\not\!\!E_T$ between 35 GeV and 85 GeV, depending on the separation in azimuth between the leading muon and $\not\!\!E_T$. The shape of these contour cuts is shown in Figure 2.

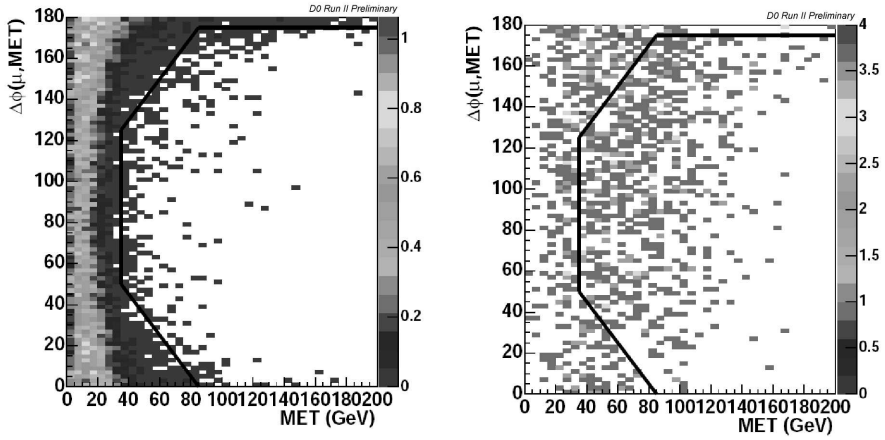

(a) (b)

FIG. 2: $\not\!\!E_T$ contour cut (in black) applied to Monte Carlo (a) $t\bar{t}$ signal and (b) WWjj background in the $\mu\mu$ channel.

In the $e\mu$ channel, a cut on the "electron likelihood" is used in place of the electron likelihood fit described in [3]. The electron likelihood for a candidate electron is formed from a combination of:

- f_{EM}, the fraction of the candidate's energy deposited in the electromagnetic calorimeter,
- a χ^2 fit on the match between the calorimeter cluster and a central track,
- the distance of closest approach of the candidate to the beamline,
- the ratio of tranverse energy in the calorimeter cluster to the tranverse momentum of the matched central track, and
- the size and number of tracks in a cone around the electron candidate.

This likelihood variable distinguishes between electrons from physics process (which have a likelihood value near 1), and "fake" electron signals from pions (which have a value near 0).

Electrons with electron likelihood values less than 0.25 are rejected for the $e\mu$ mass analysis. This dramatically reduces the background from fake electrons, while only minimally reducing the selection efficiency on real electrons, as shown in Figure 3. A missing tranverse energy cut of 25 GeV is also applied, and the cut on the combined H_T^ℓ from the jets and leading lepton is increased from 122 GeV to 140 GeV in order to reduce background from physics events.

Events which pass all selection cuts are then required to have at least one solution in the event-weighting scheme detailed in Section I. In that scheme, each neutrino momentum is obtained from the solution to a quadratic equation. Thus, it is possible that the solved momentum for one or both neutrinos is imaginary. In some events, there is no choice of top mass or neutrino rapidity that yields a real solution for both neutrinos. This happens rarely for MC top events, at the level of 0.2% or so. It happens more frequently for background events, and roughly 4% of background events are found to yield no real solution. The requirement of at least one real event weight solution acts as a *de facto* additional cut on the selected events, further reducing the expected event yield. Of the 22 events that pass the kinematic selection cuts, 1 event (in the $\mu\mu$ channel) fails to produce any real solution. The distribution of the remaining 21 events is shown in Table I, along with the expected number of signal and background events in each of the dilepton channels.

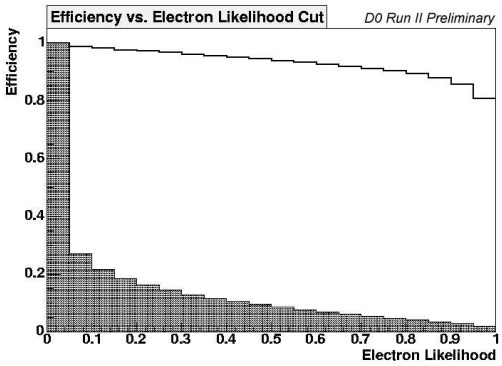

FIG. 3: Efficiency on electron candidates from (unshaded) $t\bar{t}$ and (shaded) QCD events as a function of electron likelihood.

TABLE I: Expected and observed yields for signal and background in the $e\mu$, ee, and $\mu\mu$ decay channels, after all selection cuts are applied.

$e\mu$		ee		$\mu\mu$	
Source	Expected Yield	Source	Expected Yield	Source	Expected Yield
$t\bar{t} \rightarrow e\mu$	9.79	$t\bar{t} \rightarrow ee$	3.49	$t\bar{t} \rightarrow \mu\mu$	2.53
		$Z \rightarrow ee$	0.43 ± 0.14	$Z \rightarrow \mu\mu$	0.91 ± 0.13
$Z \rightarrow \tau\tau$	0.70 ± 0.16	$Z \rightarrow \tau\tau$	$0.29^{+0.10}_{-0.13}$	$Z \rightarrow \tau\tau$	0.06 ± 0.02
WW/WZ	0.71 ± 0.26	WW/WZ	$0.19^{+0.11}_{-0.14}$	WW/WZ	0.19 ± 0.03
EM fakes	0.31 ± 0.28	EM fakes	0.09 ± 0.03	Muon fakes	0.13 ± 0.03
Total	11.32 ± 0.41	Total	$4.49^{+0.41}_{-0.47}$	Total	3.82 ± 0.16
Observed	**15**	**Observed**	**5**	**Observed**	**1**

IV. TEMPLATES

Each selected event has an event weight distribution generated from the weighted neutrino solutions. The widths of these distributions indicate that they may be re-binned into coarse, 25-GeV bins with no loss of information, as shown in Figure 4. This reduces the number of bins from 125 to 10. Normalizing the total event weight of each event to unity adds another constraint, allowing each event to be characterized by a 9-dimensional vector of event weights.

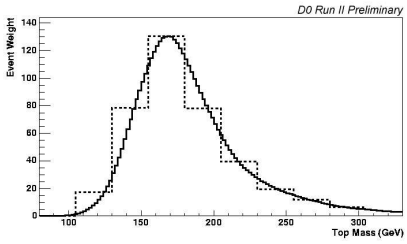

FIG. 4: Sum of event weight distributions for Monte Carlo samples of $t\bar{t} \rightarrow e\mu$ events with top mass of 175 GeV. Event weight distributions are shown before (black) and after (red) re-binning.

Event weight vectors are also generated for Monte Carlo samples of $t\bar{t}$ to dilepton decays for various top quark masses. Each Monte Carlo sample contains events that were generated with ALPGEN [5]. Fragmentation and hadronization were modeled with PYTHIA [6], as were decays of short-lived particles. A full detector simulation was provided with GEANT [7].

Nineteen independent Monte Carlo samples exist, for top quark masses ranging from 120 GeV to 230 GeV. Event weight vectors are generated for all events that pass the selection criteria described in Section II. The collection of all weight vectors

for a given mass constitutes a "template" to which weight vectors from data may be compared.

Event weight vectors are generated for background events as well as for signal events. Monte Carlo events are used for physics background processes, while fake processes are modeled from data events with loosened selection criteria. The number of events selected from background processes tends to be low, so larger samples are generated using a fast parameterized detector simulation. These samples are used for an estimate of systematic error, as described in section VI A.

V. MAXIMUM LIKELIHOOD

Each individual event weight vector $\vec{w}_{ev}$ from data is compared to weight vectors $\vec{w}_i$ from the MC templates. An estimate of the signal probability density f_s is made by placing a Gaussian kernel of width h at the event weight of each MC event, so that:

$$f_s(\vec{w_{ev}} \mid m_t) = \frac{1}{N_{MC}(m_t)} \sum_{i=1}^{N_{MC}(m_t)} \prod_{j=1}^{9} \frac{e^{[\frac{-(w_{ev,j}-w_{i,j})^2}{2h^2}]}}{\int_0^1 e^{[\frac{-(w-w_{i,j})^2}{2h^2}]} dw}. \tag{2}$$

A similar estimate is made of the background probability density. In the case where there are multiple background sources, each source is scaled by a relative weight vector $\vec{b}$, which is defined by the expected number of background events $\bar{n}_k$ for each background k and the number of Monte Carlo weight vectors for each background:

$$\frac{b_k N_k^{MC}}{\sum_{k=1}^{N_{\text{source}}} b_k N_k^{MC}} = \frac{\bar{n}_{b,k}}{\sum_{k=1}^{N_{\text{source}}} \bar{n}_{b,k}}. \tag{3}$$

The probability density estimate (PDE) for the background may thus be written as:

$$f_b(\vec{w_{ev}}) = \frac{1}{\sum_{k=1}^{N_{source}} b_k N_k^{MC}} \sum_{k=1}^{N_{source}} b_k \sum_{i=1}^{N_{k,MC}} \prod_{j=1}^{9} \frac{e^{[\frac{-(w_{ev,j}-w_{ik,j})^2}{2h^2}]}}{\int_0^1 e^{[\frac{-(w-w_{ik,j})^2}{2h^2}]} dw}. \tag{4}$$

A likelihood function is formed at each mass point by combining the signal and background PDEs with the number of signal (n_s) and background (n_b) events. A Gaussian constraint $g(n_b, \bar{n}_b, \sigma_b)$ forces consistency between the observed and expected number of background events, and a Poisson constraint $p(n_s + n_b, N)$ ensures agreement between the observed number of events N and the sum of n_s and n_b. The combined likelihood function is thus:

$$L(\vec{w_{ev}}, \bar{n_b}, N \mid m_t, n_s, n_b) = g(n_b, \bar{n}_b, \sigma_b) p(n_s + n_b, N) \prod_{i=1}^{N} \frac{n_s f_s(\vec{w}_i \mid m_t) + n_b f_b(\vec{w}_i)}{n_s + n_b}. \tag{5}$$

The values of n_s and n_b at each Monte Carlo top mass are allowed to fluctuate, and the likelihood function is minimized with respect to these variables at each mass. A quadratic fit is performed on the minimized points, and an overall minimum is determined from the fit. It can be shown that, in the limit of infinite statistics, the 68% confidence interval is defined by the region in which the negative logarithm of the likelihood varies by less than half a unit from its minimum value [8].

The utility of this likelihood fitter is tested by performing ensemble tests from samples of Monte Carlo signal and background weight vectors. For each dilepton channel, a set of N weight vectors is chosen, where N is the number of observed events in the given channel. The weight vectors are chosen randomly from Monte Carlo signal or background template files, so that the average number of background events per source matches the expected average background. Likelihoods are calculated for the sets of events in each channel, and a parabolic fit is then performed over the negative logarithm of the combined likelihoods ($-\ln L$). An estimation of the statistical uncertainty is made by calculating the masses at which the $-\ln L$ value is half a unit above its maximum. Figure 5 shows the good agreement between the output minima and input mass, and that the widths of pull distributions are near their expected value of 1.0. The fit line in Figure 5a is used as a calibration tool on the results from data, mapping the output minimum to an input top quark mass.

The parameter h is a free parameter that sets the width of the Gaussian kernel. The value of h in this analysis is determined *apriori* from ensemble tests. Further ensemble tests are also performed on differing fit ranges around the minimum, as shown in Figure 6. The results of these tests show the best agreement between output minima and input masses for a value of $h = 0.15$ and a fit range of $\pm$ 20 GeV about the fit minimum. Ensemble tests were also performed using fits that were cubic rather than quadratic, but it was found that those fits reduced the number of fits with good solutions without improving the agreement between output and input.

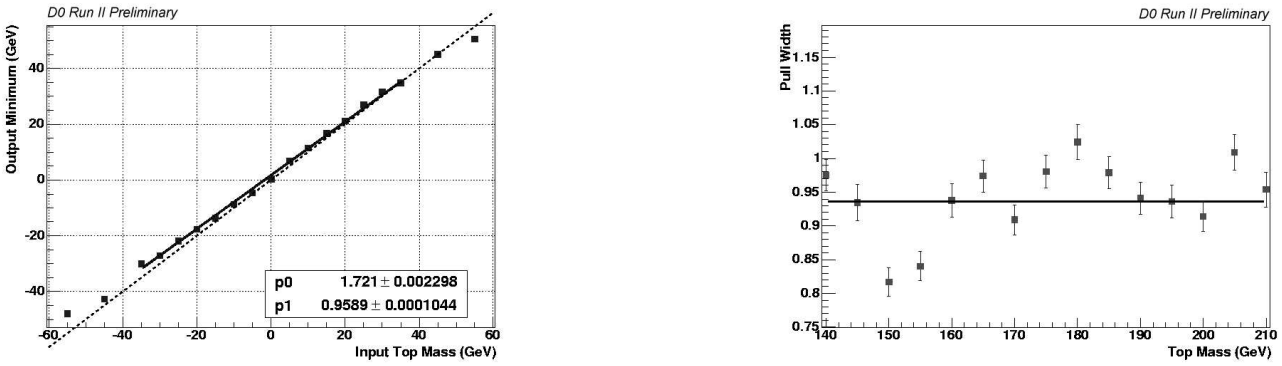

(a) (b)

FIG. 5: Ensemble tests of average likelihood minimum vs. input top mass. Each point consists of 1000 ensembles of 21 dilepton events each, with 15 events from the $e\mu$ sample, 5 from the ee sample, and 1 from the $\mu\mu$ sample. The dashed line in plot (a) represents perfect agreement between the input mass and output minimum, while the solid line in plot (b) represents the average pull width over all masses.

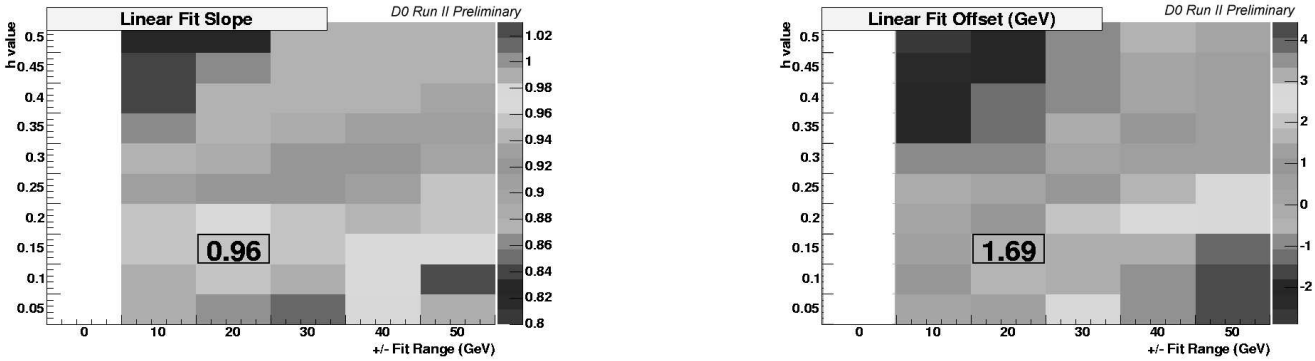

(a) (b)

FIG. 6: Results of ensemble tests on the (a) slope and (b) offset of linear fits to the likelihood minima for various values of fit range and smearing parameter h, using ensembles of 15 $e\mu$ events, 5 ee events, and 1 $\mu\mu$ event. The boxed values indicate the slope and offset values for the fit range and h value used in the analysis. The highlighted values differ slightly from those in Figure 5 due to ensemble fluctuations.

VI. RESULTS

The results of the likelihood fits for the ee, $e\mu$, and $\mu\mu$ channels are shown in Figure 7. At each top quark mass point, data event weight distributions are compared to Monte Carlo background event templates and the Monte Carlo signal template for that particular mass. Prior to MC event selection, a correction factor of 1.034 is applied to all jets to account for differences between Monte Carlo and data [10].

The minima of the likelihoods for the three individual channesl are 148 ± 11 GeV for the $e\mu$ channel, 194 ± 17 GeV for the ee channel, and 183 ± 34 GeV for the $\mu\mu$ channel. The widths include statistical effects only and are determined by finding the points at which the quadratic fit to the likelihood points rises by half a unit from its minimum. The large width for the $\mu\mu$ channel is due to the fact that only a a single event passes the selection for that channel, while the expected number of background events for that channel is greater than one. When the likelihoods for all three channels are combined, the minimum is at 178 GeV, as shown in Figure 8. Converting the position of the miminum to a top quark mass measurement by applying the linear calibration from Figure 5 yields a result of 175.6 ± 10.7 (stat) GeV.

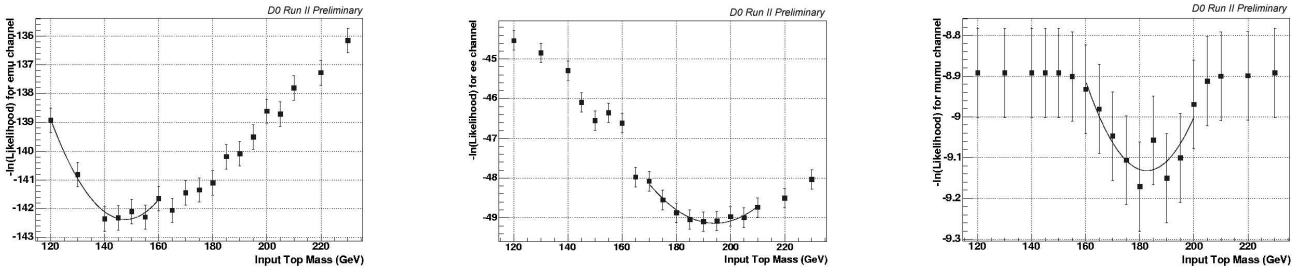

(a) (b) (c)

FIG. 7: -ln (Likelihood) minima vs. mass for the (a) $e\mu$, (b) ee, and (c) $\mu\mu$ channels.

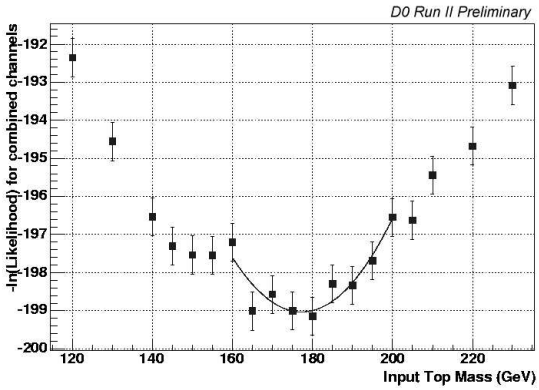

FIG. 8: -ln (Likelihood) minima vs. mass for the combined dilepton channels.

A. Statistical Uncertainties

The statistical uncertainties quoted above are calculated from the quadratic fit to the likelihood minima. The distribution of expected statistical errors for the ee, $e\mu$, and combined dilepton channels are shown in Figure 9. Seventy-five percent of the ensemble tests over the combined channels produced statistical errors less than the observed statistical error of 110.7 GeV.

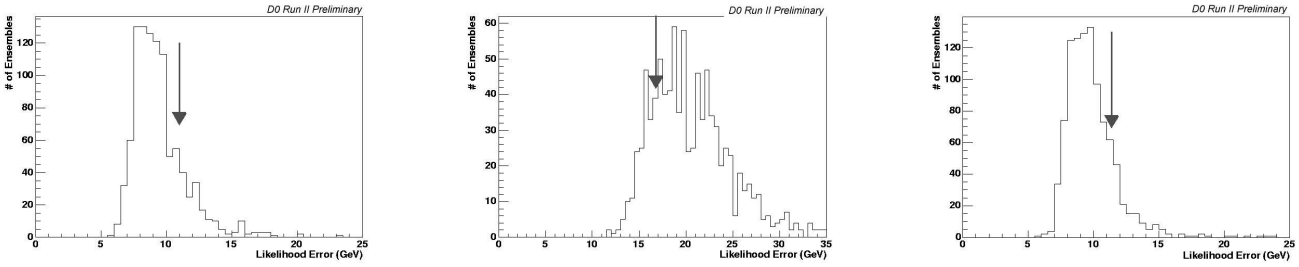

(a) (b) (c)

FIG. 9: Distribution of expected statistical errors from 1000 ensemble tests on the (a) $e\mu$, (b) ee, and (c) combined $ee+e\mu+\mu\mu$ channels. The distribution of errors for a single $\mu\mu$ event varies wildly, and is not shown here. The arrows indicate the statistical error from the fit over data in each of the channels.

B. Systematic Uncertaintiess

Systematic uncertainties due to object resolution uncertainties are found by varying the objects' momenta by $\pm 1\sigma$, repeating the event selection for the new objects, and comparing ensembles of the new object event distributions with templates made from the original events. This approach is also used to estimate systematic uncertainties from uncertainties in jet energy scale and the modeling of gluon radiation. A summary of all such systematics is given below.

- Jet energy scale. Systematic uncertainties in jet energy scale arise from the following factors:
  - A 3.4% uncertainty in light quark jet energies [9],
  - An additional uncertainty of 2.1% due to light quark/b-quark corrections [10],
  - p_T-dependent uncertainties of 1%, and
  - η-dependent correction uncertainties of 1.4%.

  These uncertainties are added in quadrature to give an overall jet energy uncertainty of 4.4%. Jets in each Monte Carlo sample are raised and lowered by this amount, and the change in top quark mass for an input mass of 175.6 GeV is found to be $^{+5.3}_{-3.4}$ GeV. The larger of these two values is taken as the jet energy scale systematic uncertainty.

- *Jet resolution*. Jets from a Monte Carlo sample with $m_{\rm top}$=175 GeV are smeared by $\pm 1\sigma$, where σ is the width of the measured jet resolution distribution. Event selection is performed on the smeared events, and event weights are generated for the selected events. These weights are compared to the original Monte Carlo templates.

- *Muon resolution*. As with the jets, muons from a Monte Carlo sample with $m_{\rm top}$=175 GeV are smeared by $\pm 1\sigma$ of their resolution. Again, event weights are generated from events selected from the smeared samples, and are compared to the original Monte Carlo templates.

- *Gluon radiation*. Events with an extra jet are selected from a signal Monte Carlo sample of $t\bar{t}$+1 jet events with $m_{\rm top}$=175 GeV. Only events with exactly three jets are chosen from this sample. These events are compared with templates from a subset of the original Monte Carlo templates containing only events with exactly two jets. The resulting difference between 2-jet and 3-jet events is then scaled by 32%, which is the expected fraction of events with an extra jet. Uncertainties due to events with two extra jets are estimated by doubling the difference between the 2-jet and 3-jet samples, and scaling that difference by the 8% expected contribution of $t\bar{t}$+2 jet events.

- *Parton distribution function (PDF)*. Templates are generated from a variety of $m_{\rm top}$=175 GeV samples created with leading-order and next-to-leading-order PDFs, as well as the nominal CTEQ5M PDF used for Monte Carlo event generation. Basic event selection is applied by cutting on jet and lepton energy and on $\not\!\!E_T$. Ensemble tests are performed using the new samples, and the systematic error is estimated by taking half the largest output fit difference between two samples.

- *Background shape*. Uncertainties due to the low statistics in the background templates are measured by creating separate large samples with a fast parameterized detector simulation, and repeating the ensemble tests with the large samples in place of the original background templates.

A final systematic due to the finite statistics of the signal templates is estimated by breaking the signal templates into smaller sub-templates, and comparing an ensemble of events to each of the sub-templates. The variance of output minima from fits performed with each of the sub-templates is used as an estimate of this uncertainty.

A list of all evaluated systematic uncertainties appears in Table II. The systematic uncertaintiess are dominated by jet energy scale uncertainties. The combined systematic uncertainty is ± 6.0 GeV, and the measured mass on the dilepton channels is 175.6 ± 10.7 (stat.)± 6.0 (syst.) GeV.

TABLE II: Summary of systematic uncertainties for a combined measurement across all dilepton channels.

Source	Error (GeV)
Jet energy scale	$\pm$5.3
Jet resolution	$\pm$0.5
Muon resolution	$\pm$0.4
$t\bar{t}$+jets	$\pm$2.0
PDF variation	$\pm$0.7
Background template shape	$\pm$1.3
Template fit statistics	$\pm$0.9
Total systematic Uncertainty	$\pm$6.0

[1] V.M Abazov, et al., "The Upgraded DØ Detector," Fermilab-Pub-05/341-E (2005).

[2] Pseudorapidity η is defined in terms of the polar angle θ as $\eta(\theta) = -ln(tan(\frac{\theta}{2}))$.

[3] The DØ Collaboration, "Measurement of the $t\bar{t}$ Production Cross Section at $\sqrt{s} = 1.96$ TeV in Dilepton Final States using 370 pb^{-1} of DØ Data," DØ Note 4850-CONF.

[4] V. Barger, J. Ohnemus, and R.J.N. Phillips, Phys. Rev. D **48**, 3953 (1993).

[5] M. Mangano *et al.*, "ALPGEN, a generator for hard multiparton processes in hadronic collisions," arXiv:hep-ph/6206293.

[6] T. Sjstrand, L. Lnnblad, and Stephen Mrenna, "PYTHIA 6.2 Physics and Manual," arXiv:hep-ph/0108264.

[7] R. Brun *et al.*, "GEANT - detector description and simulation tool," CERN Program Library Vers. 3.21, W5013 (1993).

[8] A.G Frodesen, O. Skjeggstad, and H. Tøofhte, *Probability and Statistics in Particle Physics*, Universitetsforlaget (1979).

[9] M. Mulders and M. Weber, "Top Mass Measurement with b-tagging in the Lepton+Jets Channel using the Ideogram Method in Run II," DØNote 4705, under review.

[10] The DØ Collaboration, "Top Quark Mass Measurement with the Matrix Element Method in the Lepton+Jets Final State at DØ Run II," DØ Note 4874-CONF.